Supplementary Information

Mechanical unzipping and rezipping of a single SNARE complex reveals hysteresis as a force-generating mechanism

Duyoung Min, Kipom Kim, Changbong Hyeon, Yong Hoon Cho, Yeon-Kyun Shin and Tae-Young Yoon

Supplementary Figures and Tables

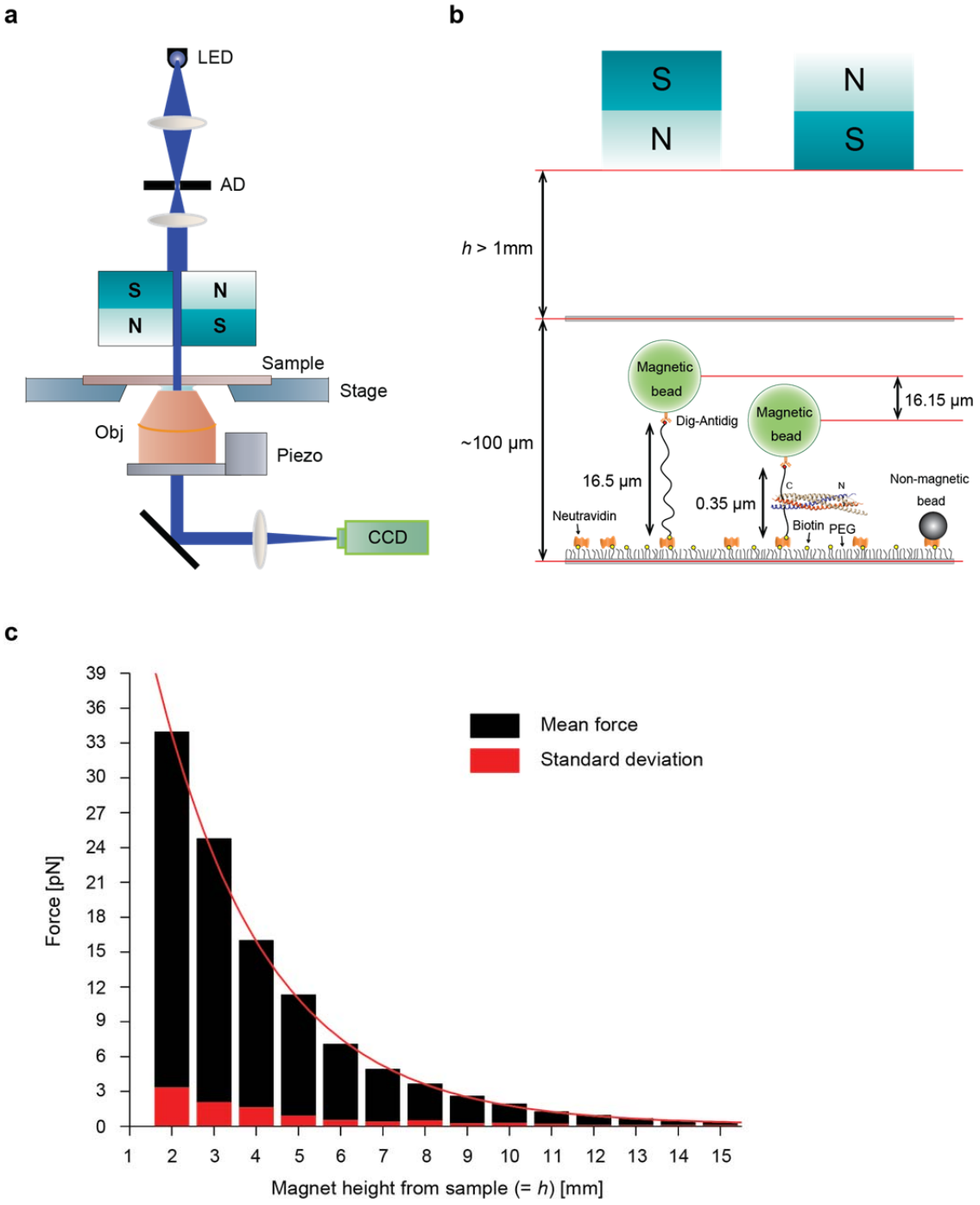

Supplementary Figure S1 | Single molecule magnetic tweezers and force calibration. (**a**) Single-molecule magnetic tweezers consists of a LED light source, a pair of magnet, a custom-built inverted microscope, a nano-positioner for objective lens, and a CCD camera. (**b**) Sample schematic for force calibration. The SNARE-DNA hybrid is also shown for comparison. The forces were calibrated by

analyzing lateral fluctuations of magnetic beads, which were tethered on the surface through a 16.5-μm-long λ-DNA. It is calculated as equation [2], $F = k_B Tl / < \delta x^2 >$, where $k_B T$ is the thermal energy, l the extension of the DNA tether, and $< \delta x^2 >$ the lateral fluctuations of the bead. This λ-DNA tether is much longer than the 350-nm DNA-handles used for the main experiments but the force differences should be less than 0.16 pN (= 1 pN·(16.5–0.35 μm)/100 μm). (**c**) The calibrated forces applied to magnetic beads as a function of the magnet height from sample surface (*h*). The black and red histograms respectively represent the mean forces and the standard deviations (*n* = 10-18 molecules for each data points). To increase 1 pN, the magnet should approach the sample by 100-200 μm in the force range between 5 and 34 pN (see Supplementary Methods for details).

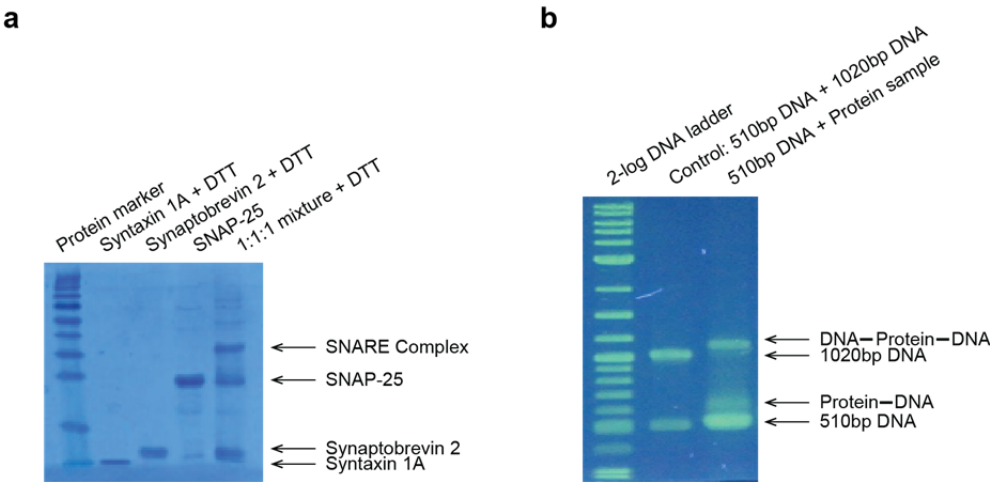

Supplementary Figure S2 | Electrophoresis analyses of SNARE proteins, SNARE complex and SNARE-DNA hybrid. (**a**) 12% SDS-PAGE showing the protein bands corresponding to syntaxin 1A, synaptobrevin 2, SNAP-25 and SNARE complex. (**b**) 1.3% TAE agarose gel shows the fluorescence bands corresponding to Protein-DNA and DNA-Protein-DNA constructs, indicating that the desired SNARE-DNA hybrid with two DNA handles were formed.

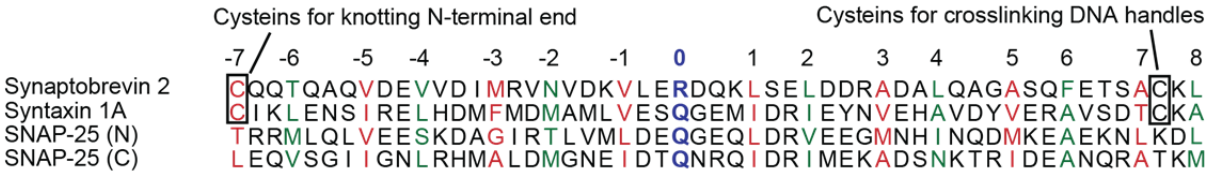

Supplementary Figure S3 | Sequences of the SNARE proteins used for C-to-N unzipping experiment. The residues in the -7 layer and adjacent to the +7 layer of syntaxin 1A and synaptobrevin 2 were mutated to cysteins, for knotting the N-terminal covalently and crosslinking DNA handles to the C-terminus of the SNARE complex, respectively.

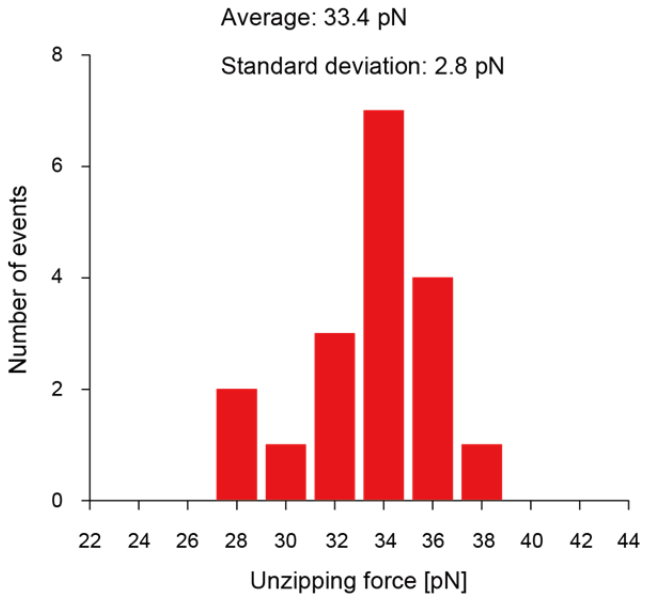

Supplementary Figure S4 | Distribution of unzipping forces. The unzipping forces for single SNARE complexes were measured while gradually increasing the tension at a loading rate of 1 pN/s, as in Figure 1c and 1d. The average force is 33.4 pN and the standard deviation is 2.8 pN (N = 18 events from n = 12 SNARE complexes).

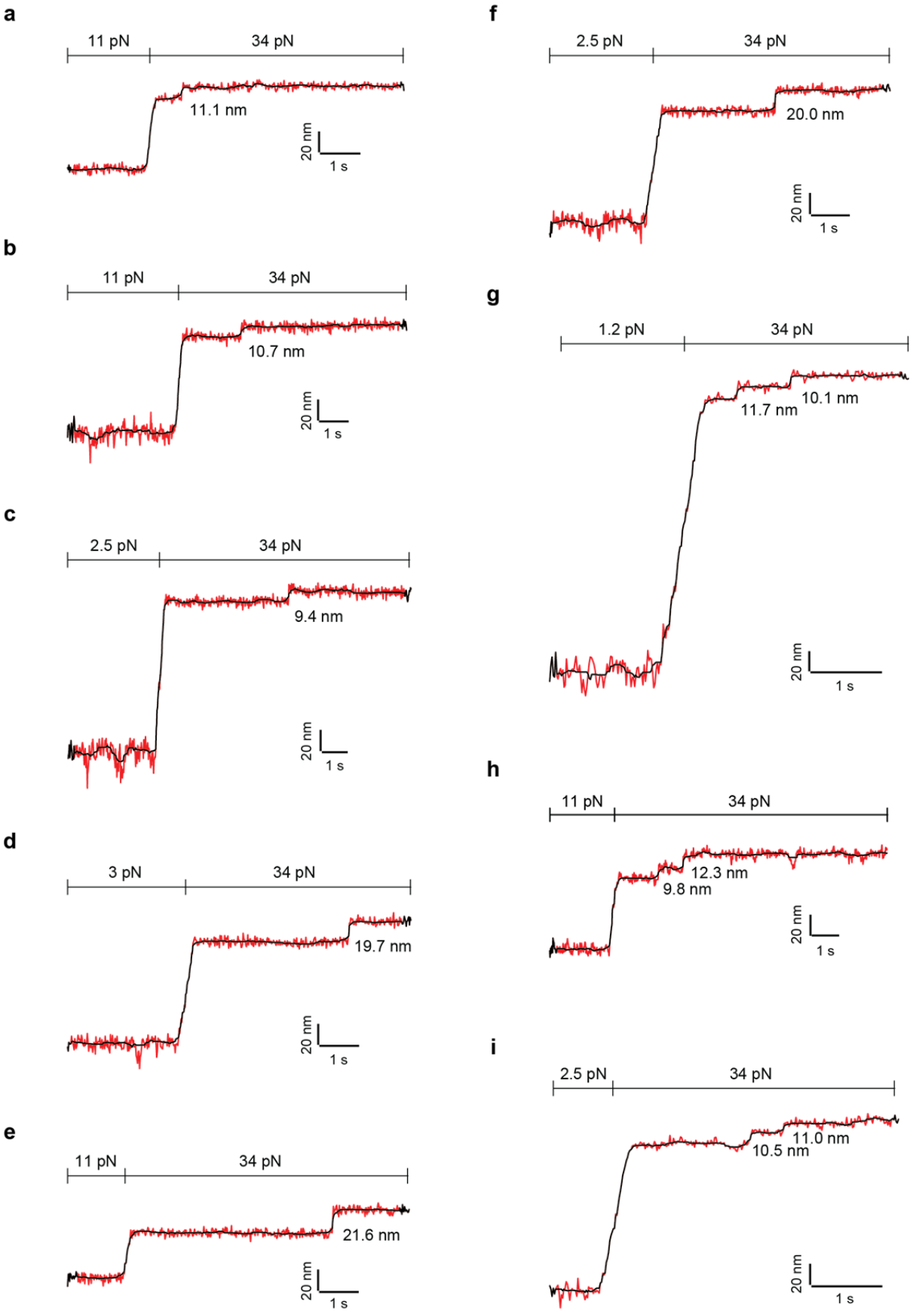
a
11 pN
34 pN
11.1 nm
20 nm
1 s
b
11 pN
34 pN
10.7 nm
20 nm
1 s
c
2.5 pN
34 pN
9.4 nm
20 nm
1 s
d
3 pN
34 pN
19.7 nm
20 nm
1 s
e
11 pN
34 pN
21.6 nm
20 nm
1 s
f
2.5 pN
34 pN
20.0 nm
20 nm
1 s
g
1.2 pN
34 pN
11.7 nm
10.1 nm
20 nm
1 s
h
11 pN
34 pN
12.3 nm
9.8 nm
20 nm
1 s
i
2.5 pN
34 pN
11.0 nm
10.5 nm
20 nm
1 s

Supplementary Figure S5 | (a-i) Additional real-time traces showing the C-to-N unzipping events of single SNARE complexes. The force was increased from 1-11 pN to 34 pN with a loading rate of 58 pN/s. The traces show one-step unzipping events with either approximately 10-nm step size (a-c) or approximately 20-nm step size (d-f), or two-step unzipping events (g-i).

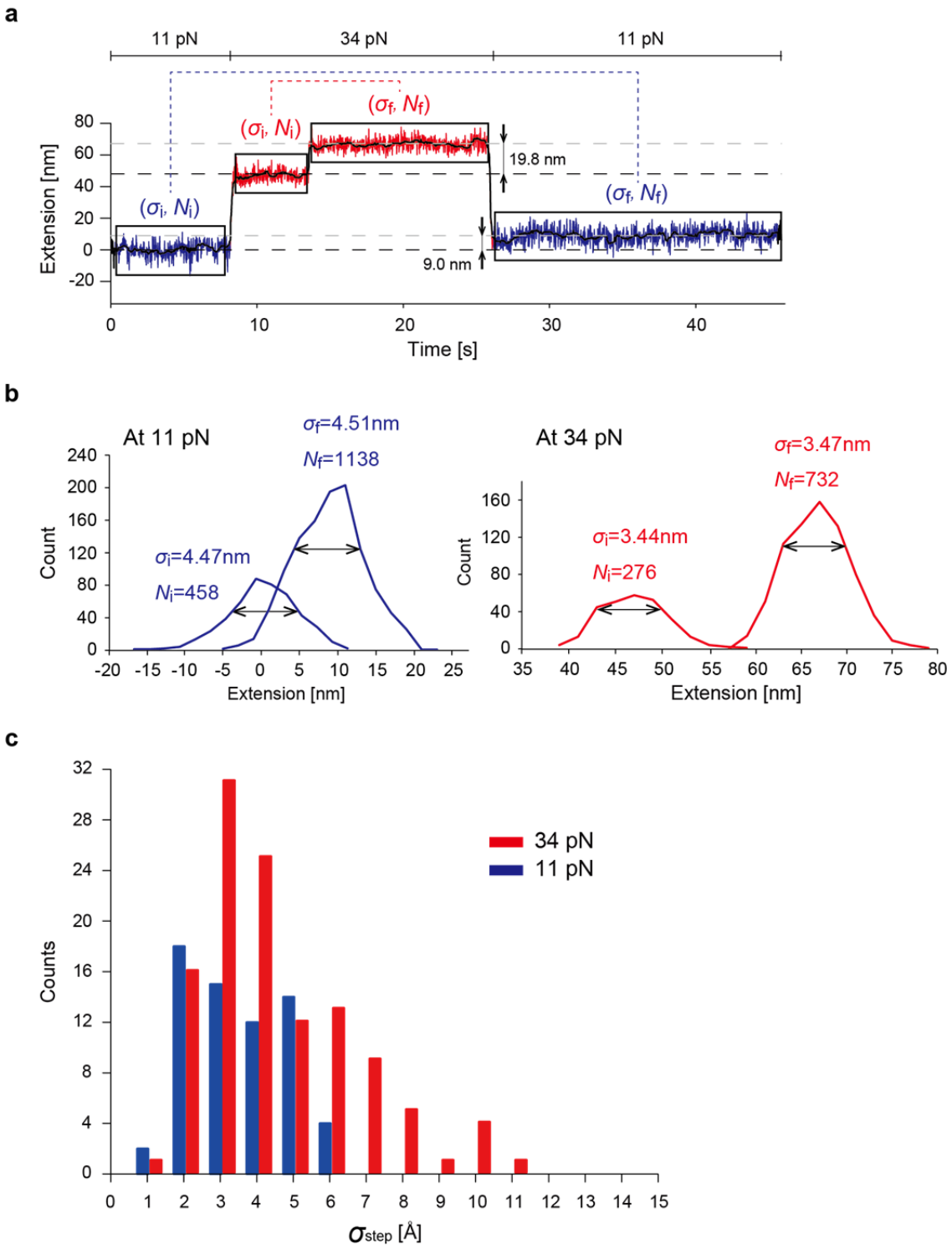

Supplementary Figure S6 | Error of step-size measurement. (a) Representative traces showing the determination of step sizes for the unzipping and rezipping events. **(b)** The error in step-size measurement (σ_{step}) is calculated as equation [S6], $\sigma_{step}{}^2 = \frac{\sigma_i{}^2}{N_i} + \frac{\sigma_f{}^2}{N_f}$, where (σ_i, σ_f) are the

standard deviations before and after the unzipping event at 34 pN (or the rezipping event at 11 pN) and (N_i, N_f) are the number of data points used for assessing the standard deviations. **(c)** Errors in step-size measurement. The unzipping events from Figure 2d (N = 119 events) were used for the 34-pN case, and the rezipping events from Figure 3e (N = 63 events) were used for the 11-pN case. The error in our step-size measurement is smaller than '1 nm' for both unzipping and rezipping events (see Supplementary Methods for details).

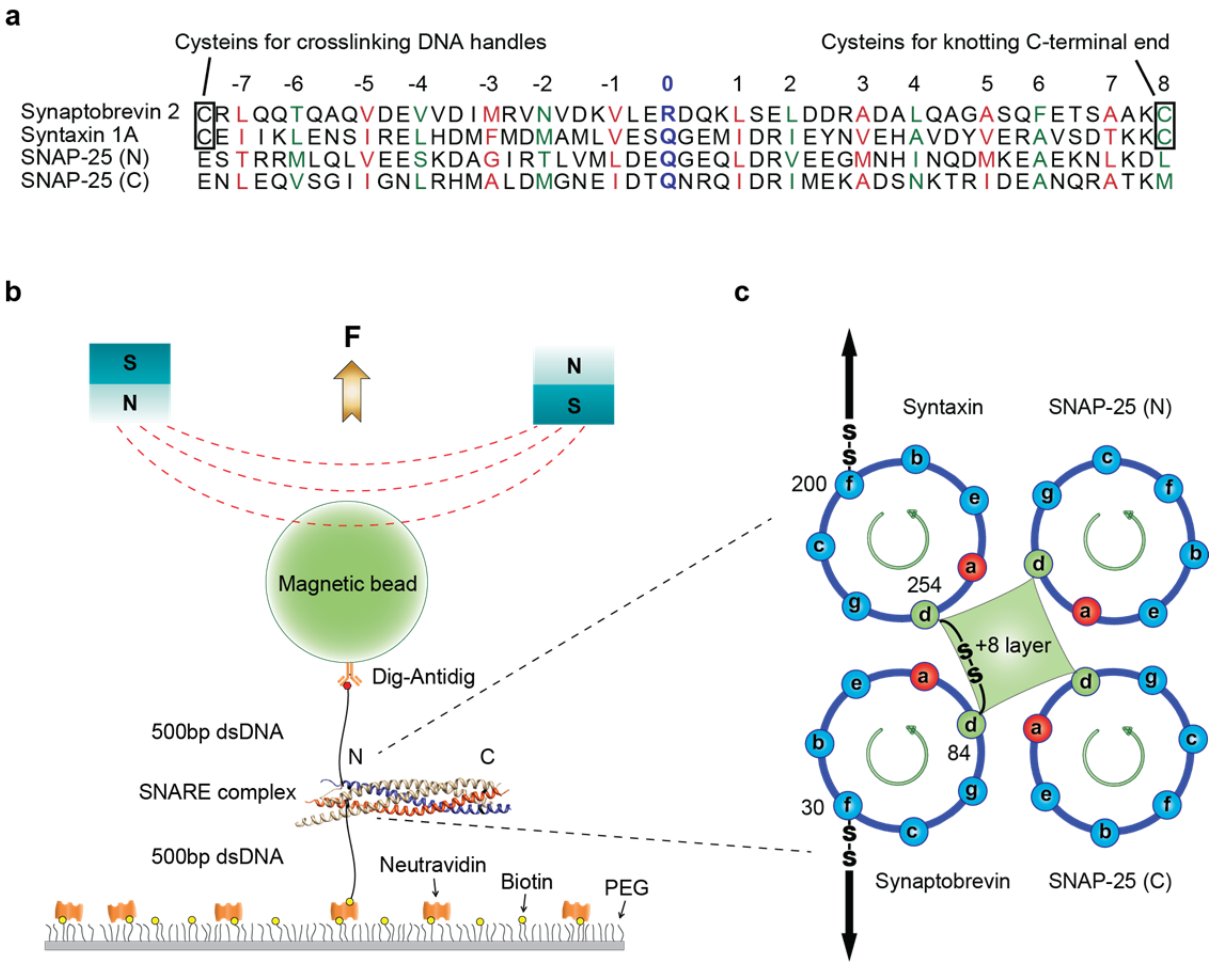

Supplementary Figure S7 | Experiment design of N-to-C unzipping experiment. (**a**) Sequences of the SNARE proteins used for the N-to-C unzipping experiment. The residues in the +8 layer and adjacent to the -7 layer of syntaxin 1A and synaptobrevin 2 were mutated to cysteins, for knotting the C-terminal covalently and crosslinking DNA handles to the N-terminus of the SNARE complex, respectively. (**b**) Experimental scheme for the N-to-C unzipping experiment (**c**) Helical wheel diagram of the SNARE complex. The f and d positions of the heptad repeats are used to attach DNA handles and knot the C-terminal.

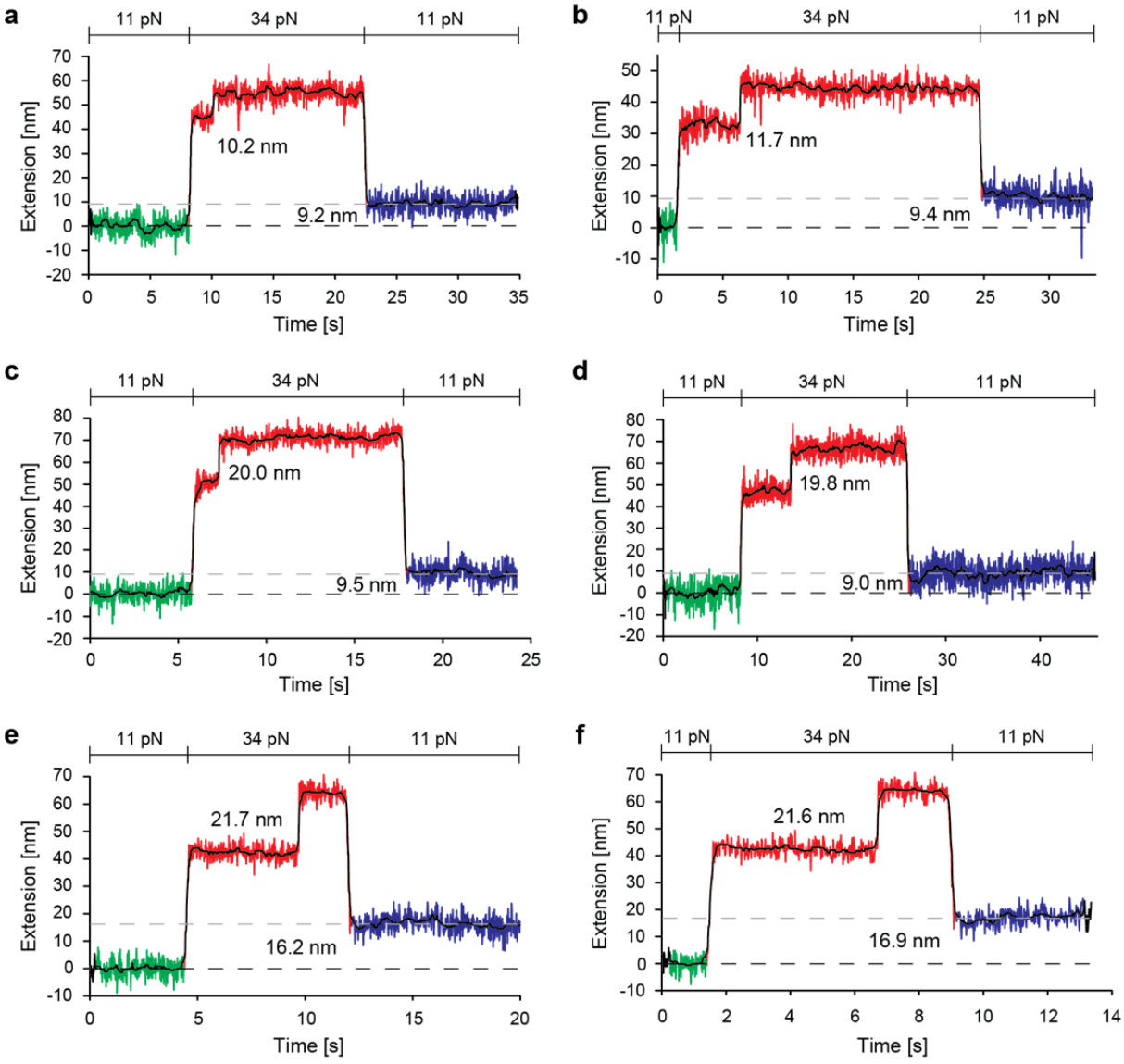

Supplementary Figure S8 | (a-f) Additional real-time traces while applying cycles of the constant-force application. Fully-assembled SNARE complexes at 11 pN (green traces) were unzipped by application of the 34-pN force (red traces). When the force was lowered back to 11 pN (blue traces), the extensions were higher than those observed before 34-pN unzipping.

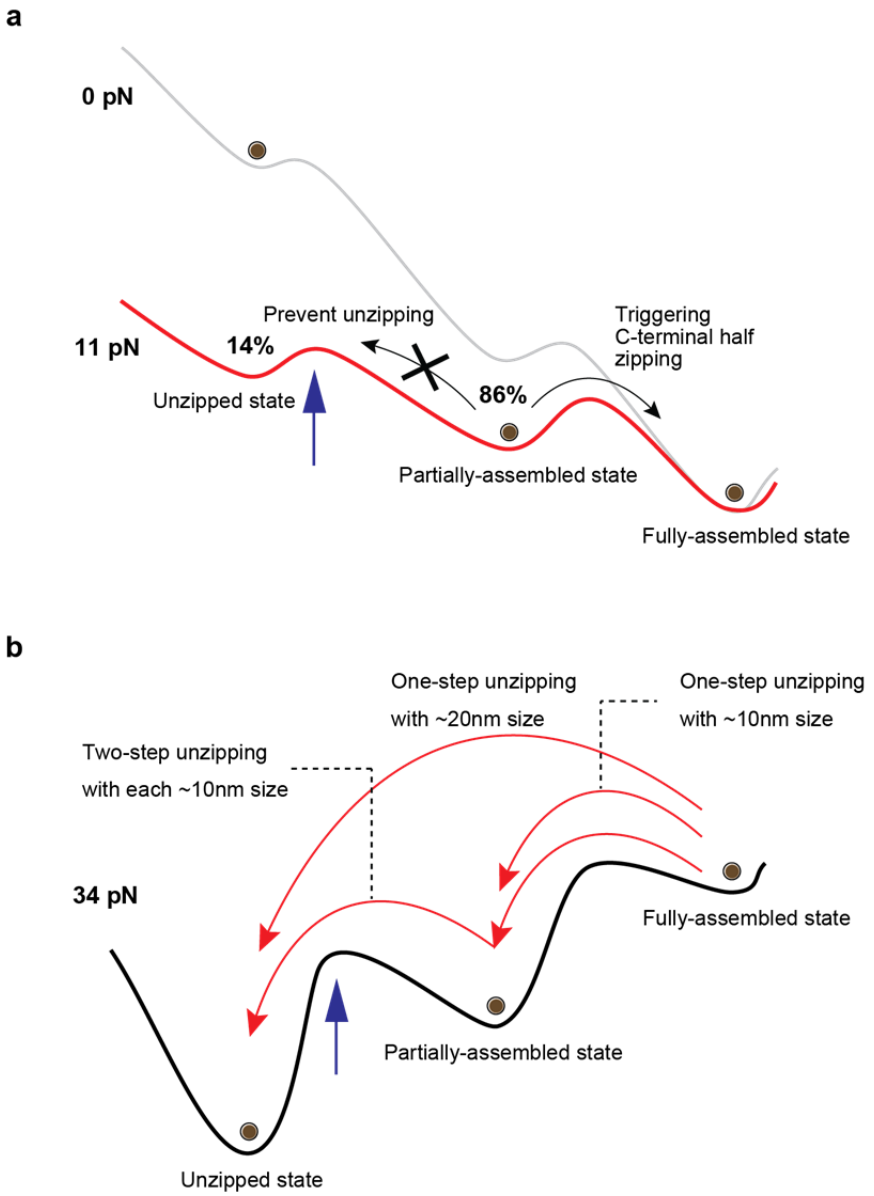

Supplementary Figure S9 | (a and b) Energy landscape diagrams for the SNARE-complex formation at 0-pN and 11-pN force (a), at 34-pN force (b). (a) If we use the zippering of the -5 layer as a criterion for partial zippering, which corresponds to the extension difference (*D*) of approximately 15 nm, 86% are partially zipped and 14% still remain in the unzipped state. 14% of the rezipping processes failed to cross the first barrier (blue arrow), trapped in the unzipped state. The other 86% of the rezipping processes were all blocked by the second energy barrier and stalled in the partially-assembled state (note that no population at *D*=0 in Fig. 3e). **(b)** The first barrier (blue arrow) halts the mechanical unzipping process (at 34 pN) at the middle layers, producing partial-unzipping events observed in Figure 2.

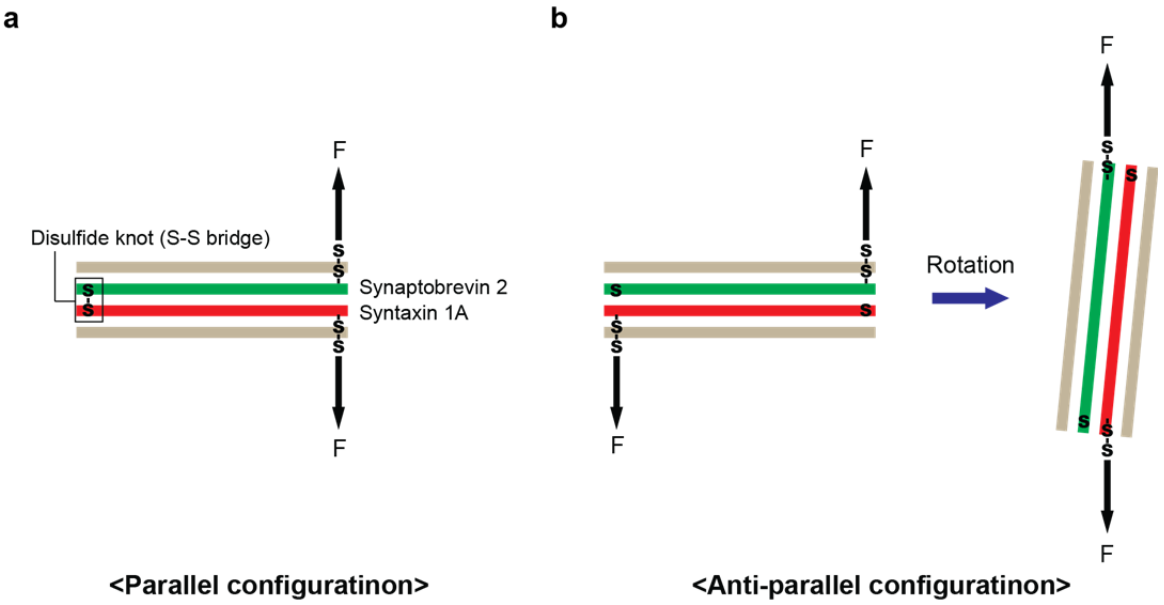

Supplementary Figure S10 | (a and b) Schematics for pulling a parallel SNARE complex (a) and an anti-parallel SNARE complex (b).

Layer	The number of unzipped residues	Contour lengths of synaptobrevin [nm]	Extensions of synaptobrevin at 34 pN [nm]	Extensions of precomplex [nm]	Extensions of SNARE complex at 34 pN [nm]
+6	5	1.9	1.486	0.831	**1.269**
+5	8	3.04	2.377	1.203	**2.532**
+4	12	4.56	3.566	1.797	**4.315**
+3	15	5.7	4.457	2.220	**5.629**
+2	19	7.22	5.646	2.825	**7.423**
+1	22	8.36	6.537	3.264	**8.753**
0	26	9.88	7.726	3.879	**10.557**
-1	29	11.02	8.617	4.225	**11.794**
-2	33	12.54	9.806	4.813	**13.571**
-3	36	13.68	10.697	5.271	**14.92**
-4	40	15.2	11.886	5.844	**16.682**
-5	43	16.34	12.777	6.296	**18.025**
-6	47	17.86	13.966	6.864	**19.782**
-7	50	19	14.857	7.326	**21.135**

Supplementary Table S1 | Estimated SNARE-complex extensions for C-to-N unzipping process at 34 pN with the t-SNARE precomplex structure preserved. When a SNARE complex is unzipped from the C-terminal DNA anchor position up to a specific layer, the total extension is estimated as the sum of the extensions caused by synaptobrevin 2 and precomplex, which is then subtracted by 1.048 nm, the distance between the C-terminal DNA anchor residues. The extension of synaptobrevin 2 is calculated using equation [S1] of the WLC model and the precomplex extension is estimated as the layer-to-layer distance determined from the crystal structure of the SNARE complex. The extension values for the zeroth layer (ionic layer) and knotted layer are shown in red.

Layer	The number of unzipped residues	Contour lengths of synaptobrevin [nm]	Extensions of synaptobrevin at 34 pN [nm]	Extensions of precomplex [nm]	Extensions of SNARE complex at 34 pN [nm]
-6	3	1.14	0.891	0.511	**0.638**
-5	7	2.66	2.080	1.042	**2.358**
-4	10	3.8	2.971	1.521	**3.728**
-3	14	5.32	4.160	2.081	**5.477**
-2	17	6.46	5.051	2.574	**6.861**
-1	21	7.98	6.240	3.162	**8.638**
0	24	9.12	7.132	3.585	**9.953**
+1	28	10.64	8.320	4.138	**11.694**
+2	31	11.78	9.212	4.624	**13.072**
+3	35	13.3	10.400	5.170	**14.806**
+4	38	14.44	11.292	5.647	**16.175**
+5	42	15.96	12.480	6.176	**17.892**
+6	45	17.1	13.372	6.647	**19.255**
+7	49	18.62	14.560	7.207	**21.003**
+8	52	19.76	15.452	7.666	**22.354**

Supplementary Table S2 | Estimated SNARE-complex extensions for N-to-C unzipping process at 34 pN with the t-SNARE precomplex structure preserved. When a SNARE complex is unzipped from the N-terminal DNA anchor position up to a specific layer, the total extension is estimated as the sum of the extensions caused by synaptobrevin 2 and precomplex, which is then subtracted by 1.342 nm, the distance between the N-terminal DNA anchor residues. The extension of synaptobrevin 2 is calculated using equation [S1] of the WLC model and the precomplex extension is estimated as the layer-to-layer distance determined from the crystal structure of the SNARE complex. The extension values for the zeroth layer (ionic layer) and knotted layer are shown in red.

Layer	The number of unzipped residues	Contour lengths of each unfolded protein [nm]	Extensions of each unfolded protein at 34 pN [nm]	Extensions of SNARE complex at 34 pN [nm]
+6	5	1.9	1.486	**1.924**
+5	8	3.04	2.377	**3.706**
+4	12	4.56	3.566	**6.084**
+3	15	5.7	4.457	**7.866**
+2	19	7.22	5.646	**10.244**
+1	22	8.36	6.537	**12.026**
0	26	9.88	7.726	**14.404**
-1	29	11.02	8.617	**16.186**
-2	33	12.54	9.806	**18.564**
-3	36	13.68	10.697	**20.346**
-4	40	15.2	11.886	**22.724**
-5	43	16.34	12.777	**24.506**
-6	47	17.86	13.966	**26.884**
-7	50	19	14.857	**28.666**

Supplementary Table S3 | Estimated SNARE-complex extensions for C-to-N unzipping process at 34 pN with unstructured t-SNARE proteins. When a SNARE complex is unzipped from the C-terminal DNA anchor position up to a specific layer, the total extension is estimated as the sum of the extensions caused by synaptobrevin 2 and now unstructured syntaxin 1A, which is then subtracted by 1.048 nm, the distance between the C-terminal DNA anchor residues. The extension of the unstructured syntaxin 1A is calculated in the same way as that used for synaptobrevin 2. The extension values for the zeroth layer (ionic layer) and knotted layer are shown in red.

Layer	The number of unzipped residues	Contour lengths of each unfolded protein [nm]	Extensions of each unfolded protein at 34 pN [nm]	Extensions of SNARE complex at 34 pN [nm]
-6	3	1.14	0.891	**0.440**
-5	7	2.66	2.080	**2.818**
-4	10	3.8	2.971	**4.600**
-3	14	5.32	4.160	**6.978**
-2	17	6.46	5.051	**8.760**
-1	21	7.98	6.240	**11.138**
0	24	9.12	7.132	**12.922**
+1	28	10.64	8.320	**15.298**
+2	31	11.78	9.212	**17.082**
+3	35	13.3	10.400	**19.458**
+4	38	14.44	11.292	**21.242**
+5	42	15.96	12.480	**23.618**
+6	45	17.1	13.372	**25.402**
+7	49	18.62	14.560	**27.778**
+8	52	19.76	15.452	**29.562**

Supplementary Table S4 | Estimated SNARE-complex extensions for N-to-C unzipping process at 34 pN with unstructured t-SNARE proteins. When a SNARE complex is unzipped from the N-terminal DNA anchor position up to a specific layer, the total extension is estimated as the sum of the extensions caused by synaptobrevin 2 and now unstructured syntaxin 1A, which is then subtracted by 1.342 nm, the distance between the N-terminal DNA anchor residues. The extension of the unstructured syntaxin 1A is calculated in the same way as that used for synaptobrevin 2. The extension values for the zeroth layer (ionic layer) and knotted layer are shown in red.

Layer	The number of unzipped residues	Contour lengths of synaptobrevin [nm]	Extensions of synaptobrevin at 11 pN [nm]	Extensions of precomplex [nm]	Extensions of SNARE complex at 11 pN [nm]
+6	5	1.9	1.131	0.831	**0.912**
+5	8	3.04	1.81	1.203	**1.963**
+4	12	4.56	2.716	1.797	**3.463**
+3	15	5.7	3.394	2.220	**4.564**
+2	19	7.22	4.300	2.825	**6.075**
+1	22	8.36	4.978	3.264	**7.192**
0	26	9.88	5.884	3.879	**8.713**
-1	29	11.02	6.562	4.225	**9.737**
-2	33	12.54	7.468	4.813	**11.231**
-3	36	13.68	8.146	5.271	**12.367**
-4	40	15.2	9.052	5.844	**13.846**
-5	43	16.34	9.731	6.296	**14.977**
-6	47	17.86	10.636	6.864	**16.45**
-7	50	19	11.315	7.326	**17.591**

Supplementary Table S5 | Estimated SNARE-complex extensions for C-to-N unzipping process at 11 pN with the t-SNARE precomplex structure preserved. The extension values are estimated using the same approach described in Supplementary Table S1. The extension values for the zeroth layer (ionic layer) and knotted layer are shown in red.

Supplementary Methods

Estimation on SNARE-complex extension

To map the Gaussian peaks to the corresponding structures of SNARE complex, we analyzed the extension values by using the worm-like chain (WLC) model. We first assume that synaptobrevin 2 becomes unstructured after its mechanical extraction from a single SNARE complex. This assumption seems to be reasonable because synaptobrevin has been reported many times to be intrinsically disordered in its solitary form[8-12]. Moreover, we are applying tens of pN forces (11 to 34 pN), which are large enough to disrupt any remaining alpha-helical contents. Therefore, when a SNARE complex is unzipped, extension x caused by stretching of an unstructured synaptobrevin 2 is estimated by the following WLC model in response to force f,

$$\frac{fl_{\mathrm{p}}}{k_{\mathrm{B}}T} = \frac{1}{4}\left(1-\frac{x}{l_{\mathrm{c}}}\right)^{-2} - \frac{1}{4} + \frac{x}{l_{\mathrm{c}}}, \qquad \text{[S1]}$$

where l_{c} is the contour length calculated as the number of unzipped residues times 0.38 nm (Ref. 29) and l_{p} the persistence length of 0.7 nm for the protein[28,55].

On the other hand, the structural status of syntaxin and SNAP-25 is a wholly open question, particularly after extraction of synaptobrevin 2. Therefore, we estimated the extension caused by the t-SNARE precomplex for the two extreme cases where the precomplex fully preserves its α-helical structure or the precomplex dissembles and syntaxin 1A is completely unstructured. For the first case, the extension is estimated as the layer-to-layer distance extracted from crystal structure of a SNARE complex[37,38], assuming layer-distances of SNARE complex and precomplex are almost identical. For the second case, it is estimated as stretching of an unstructured syntaxin 1A using the WLC model given in equation [S1], as in the case of synaptobrevin 2. Consequently, when a SNARE complex is unzipped from the C-terminal DNA anchor position up to the each layer at 34-pN force, the total predicted extensions are calculated as the sum of the extensions caused by synaptobrevin 2 and precomplex, which is subtracted by 1.048 nm (Ref. 37,38), the distance between the C-terminal DNA anchor residues[29,56] (Supplementary Tables S1 and S3 for both structural cases).

To gain an insight toward the structural status of syntaxin and SNAP-25, the t-SNARE precomplex, we repeated the unzipping experiment in the reverse direction, N- to C-terminal direction. For this N-to-C unzipping experiment, we attached the DNA handles next to the -7 layer and knotted the +8 layer using a disulfide bond (Supplementary Fig. S7). We carefully chose the positions of these DNA handles and disulfide bonds so that we could see an extension very similar to that of the previous C-to-N unzipping experiment when a single SNARE complex was fully unzipped. In the N-

to-C unzipping process, the total predicted extensions from the N-terminal DNA anchor position up to the each layer are also calculated as the sum of the extensions caused by synaptobrevin 2 and precomplex, minus 1.342 nm (Ref. 37,38), the distance between the N-terminal DNA anchor residues[29,56] (Supplementary Tables S2 and S4 for both structural cases).

Our model estimates that when a SNARE complex is fully unzipped, an extension of 21.1 nm is predicted for the original C-to-N unzipping experiment, which is very similar to 22.3 nm of the N-to-C unzipping experiment (Supplementary Tables S1 and S2). This estimate is based on an important assumption that the t-SNARE precomplex fully preserves its α-helical structure even after dissociation of synaptobrevin. If the t-SNARE precomplex disassembles, syntaxin would become unstructured and further stretched. The estimated extensions consequently increase to values close to 30 nm for both C-to-N and N-to-C unzipping experiments (28.7 nm and 29.6 nm, respectively) (Supplementary Tables S3 and S4). If the t-SNARE precomplex is partly unfolded, the extension would be an intermediate value between these two estimates.

The experimental data of the N-to-C unzipping experiment also show two Gaussian peaks for the first unzipping steps. We note that the higher peak is at 21.4 nm, an extension very close to 19.4 nm observed from the C-to-N unzipping experiment. Thus, for both C-to-N and N-to-C unzipping experiment, the fully-unzipped SNARE complexes consistently show the extensions at approximately 20 nm, the expected values when the t-SNARE precomplex retains its α-helicity. In the light of above discussions, we have assumed in our model that the t-SNARE precomplex and its α-helical structure is largely maintained. With these assumptions, we also estimated extensions at 11 pN for C-to-N unzipping process (Supplementary Table S5).

Extracting energy barrier parameters from the single-molecule force spectroscopy data

The survival probability $S(t)$ in Figure 4e is defined as the fraction of SNARE complexes that have remained in the partially-assembled state until time t (the force is quenched to a specific level at t = 0) (Fig. 4a-d). $S(t)$ is obtained from the first-order rate equation

$$\frac{dS(t)}{dt} = -k(t)S(t), \qquad [S2]$$

which can be transformed to $S(t) = \exp\left(-\int_0^t k(t)dt\right)$. Since $k(t)$, the kinetic constant for transition to the fully-assembled state, depends only on the force,

$$k(t) = k = k_0 \exp\left(-\frac{fx^{\ddagger}}{k_B T}\right). \qquad [S3]$$

Thus, the survival probability observed at time t is given by

$$S(t) = \exp\left(-tk_0 e^{-\frac{fx^{\ddagger}}{k_B T}} \right). \qquad [S4]$$

The survival probability after an observation time of 20 s is given as $S(20) = S_{20s} = \exp\left(-20k_0 e^{-fx^{\ddagger}/k_B T}\right)$ and finally converted to equation [1]. We fitted the experimental data in Figure 4e and 4f with these equations to obtain $x^{\ddagger}$ and k_0, where $x^{\ddagger}$ is the position of the energy barrier from the partially-assembled state confining the SNARE complex and k_0 is the kinetic rate for the zippering of the C-terminal half at zero force. The free energy of activation in the absence of external force ($\Delta G^{\ddagger}$) is extracted from the Kramers equation

$$k_0 = k_w e^{-\frac{\Delta G^{\ddagger}}{k_B T}}, \qquad [S5]$$

with the pre-exponential factor presumed to be $k_w = 1.2 \times 10^4\ s^{-1}$ (Ref. 28).

Force calibration in our magnetic tweezers apparatus

One technical advantage of the magnetic tweezers is that the force delivered to a magnetic bead, and thus to a single SNARE-DNA hybrid, can be easily controlled by changing the vertical distance of the magnets from the sample. In our apparatus, when we changed the magnet height from 8 to 2 mm, the force applied to a magnetic bead increased from 3 to 34 pN (Supplementary Fig. S1). We can presume two sources of error in these force values. Firstly, even when we precisely attain the same magnet height, the force experienced by each magnetic bead can have variations mainly due to different magnetic moments of different magnetic beads. The second source of force error is that even when we achieve the precisely the same force levels, the force levels can fluctuate in time because the magnetic beads show Brownian motion, which continuously changes the position of the magnetic beads relative to the magnet.

When we consider the physical dimensions of our magnetic tweezers apparatus, it becomes evident that we can safely rule out the second source of force error. To make 1 pN increase, the magnet should typically approach the sample by 100-200 μm (Supplementary Fig. S1c). On the other hand, the Brownian motion of the magnetic beads tethered to 1,000 base-pair DNA handles (total extension of approximately 350 nm) is typically less than 20 nm. This Brownian motion would consequently make a force fluctuation less than (20 nm/200 μm)·1 pN≈10^{-4} pN, a totally negligible value when we are dealing with the force range between 5 and 34 pN.

However, we need to do careful calibration for the first source of force error, variations of magnetic force from bead to bead. To this end, we performed an independent experiment, in which we analyzed lateral Brownian motions of different magnetic beads. The lateral Brownian motion of a magnetic bead and its variance $<\delta x^2>$ gives the direct information on force experienced by each magnetic bead through equation [2] (Ref. 21,53). To amplify the Brownian motion, we used a 16.5-μm-long λ-DNA as the DNA tether (Supplementary Fig. S1b). We note this λ-DNA tether is much longer than the 350-nm DNA handles used for the main experiments, but the force difference should be less than 0.16 pN (=1 pN·(16.5–0.35 μm)/100 μm). This force calibration experiment reveals that the force values experienced by different magnetic beads are indeed different. This force variation is, however, much smaller than the mean force value in the entire force range we studied (Supplementary Fig. S1c, black versus red bars). This is also consistent with the force calibration data from previous reports[53,57,58].

Error in the step-size determination

Our step-size measurement first determines the positions of the extension trace before and after the unzipping (or rezipping) events, and subsequently compares these positions to finally determine the step size of each event (the difference between arithmetic mean values of records over the appropriate intervals) (Supplementary Fig. S6a). This determination of the trace positions essentially corresponds to finding the peak positions of Gaussian distributions (Supplementary Fig. S6b). The relevant error is thus the standard error of the mean, which is much smaller than the standard deviation of the distribution.

To quantitatively show this, we assess the error in our step-size measurement (σ_{step}) using the equation (Ref. 59),

$$\sigma_{step}{}^2 = \frac{\sigma_i{}^2}{N_i} + \frac{\sigma_f{}^2}{N_f}. \qquad [S6]$$

This expression well illustrate that σ_{step} is a kind of standard error of the mean because the standard deviations of extension trace (σ_i, σ_f) are divided by the number of data points (N_i, N_f) used to obtain the standard deviations (e.g., see Supplementary Fig. S6a).

This means that as a larger number of data points (N_i, N_f) are included for our step-size measurement, the uncertainty can be decreased to an arbitrarily smaller level. Since the fluctuation of extension traces $(\sigma_{i,f})$ is typically 5 nm and we include more than 300 data points for each

measurement, $\sigma_{step} \approx 5\,\text{nm} / \sqrt{300} \sim 0.3\,\text{nm}$, indicating that we can estimate the step size with an accuracy down to a few Å level. Supplementary Figure S6c shows the distribution of σ_{step} showing that the error in our step-size measurement is indeed smaller than '1 nm' for both unzipping and rezipping events.

On the possibility of pulling the anti-parallel SNARE complexes

The SNARE complex can be in the 'anti-parallel' configuration[60] and moreover two DNA handles can be attached to such an anti-parallel SNARE complex as shown in Supplementary Figure S10, meaning that an extension curve can also be obtained in our magnetic tweezers experiment.

However, there are two reasons why we believe all the data are from single SNARE complexes in the parallel configuration. Firstly, if we pull an anti-parallel SNARE complex in our SNARE-DNA hybrid, we apply 'shear force' which is applied to the SNARE complex in the longitudinal direction (Supplementary Fig. S10). In order to disassemble with such a shear force, we have to break all the molecular interactions simultaneously, as opposed to the sequential unzipping of interacting residues in a parallel SNARE complex. Thus, the unzipping force for the antiparallel SNARE complex would be much higher than that for the parallel SNARE complex. But, the distribution of unzipping forces shows rather a narrow distribution around 34 pN with a standard deviation of 2.8 pN (Supplementary Fig. S4) and therefore the experiment sample is thought to be quite homogeneous. In addition, it would be difficult to expect intermediates that we observed with such a shear-force unzipping.

More importantly, in this anti-parallel configuration, there would be no 'S-S bridge' inside the SNARE complex (Supplementary Fig. S10b). Therefore, if we pull and unzip such a SNARE complex, the SNARE-DNA hybrid will be completely separated into two pieces. Obviously, we cannot observe repetitive cycles of unzipping and rezipping for the anti-parallel SNARE complex. Since we have included only the data sets that show repetitive unzipping and rezipping cycles, we assure that all the data presented in this work are obtained from the parallel SNARE complex.

Supplementary References

55 Bornschlogl, T. & Rief, M. Single molecule unzipping of coiled coils: Sequence resolved stability profiles. *Phys Rev Lett* **96**, (2006).

56 Woodside, M. T. *et al.* Nanomechanical measurements of the sequence-dependent folding landscapes of single nucleic acid hairpins. *P Natl Acad Sci USA* **103**, 6190-6195, (2006).

57 Lipfert, J., Hao, X. M. & Dekker, N. H. Quantitative Modeling and Optimization of Magnetic Tweezers. *Biophys. J.* **96**, 5040-5049, (2009).

58 Velthuis, A. J. W. T., Kerssemakers, J. W. J., Lipfert, J. & Dekkert, N. H. Quantitative Guidelines for Force Calibration through Spectral Analysis of Magnetic Tweezers Data. *Biophys. J.* **99**, 1292-1302, (2010).

59 Yildiz, A. *et al.* Myosin V walks hand-over-hand: Single fluorophore imaging with 1.5-nm localization. *Science* **300**, 2061-2065, (2003).

60 Weninger, K., Bowen, M. E., Chu, S. & Brunger, A. T. Single-molecule studies of SNARE complex assembly reveal parallel and antiparallel configurations. *P Natl Acad Sci USA* **100**, 14800-14805, (2003).